Supplementary Information

Hierarchically organized CNT@TiO_2@Mn_3O_4 nanostructures for enhanced lithium storage performance

Du-Juan Yan,[c] Xiao-Dong Zhu,[a, b,]* Ya-Chun Mao,[a] Sheng-You Qiu,[c] Liang-Liang Gu, [c] Yu-Jie Feng,[b] and Ke-Ning Sun [b,a,]*

[a]Academy of Fundamental and Interdisciplinary Sciences, Harbin Institute of Technology, Harbin 150080, China

[b]State Key Laboratory of Urban Water Resource and Environment, Harbin Institute of Technology, Harbin 150090, China

[c]Department of Chemistry, Harbin Institute of Technology, Harbin 150001, China

*Corresponding Authors.

E-mail: zxd9863@163.com, keningsunhit@126.com.

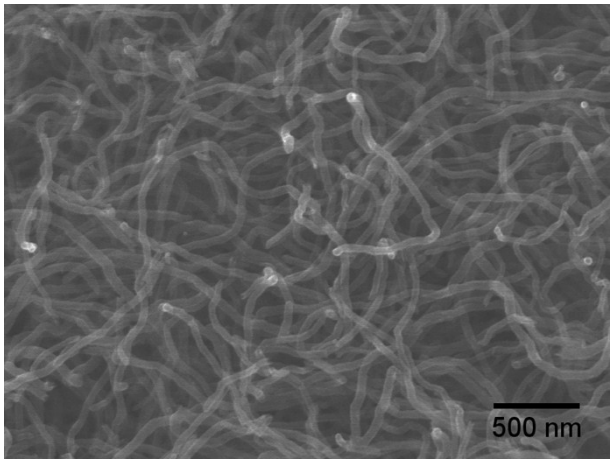

Fig. S1 – SEM image of CNTs.

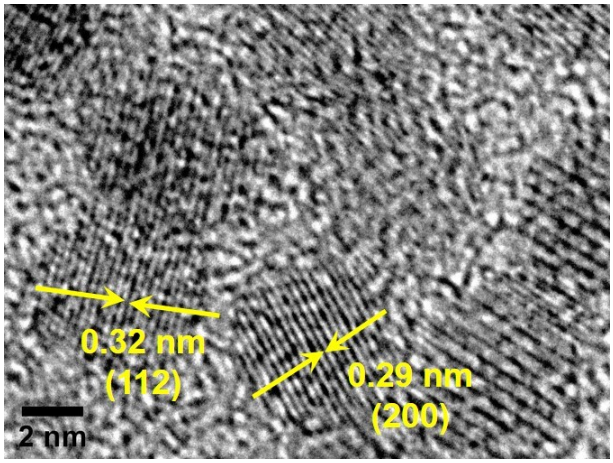

Fig. S2 – HRTEM image of Mn_3O_4 nanoparticles.

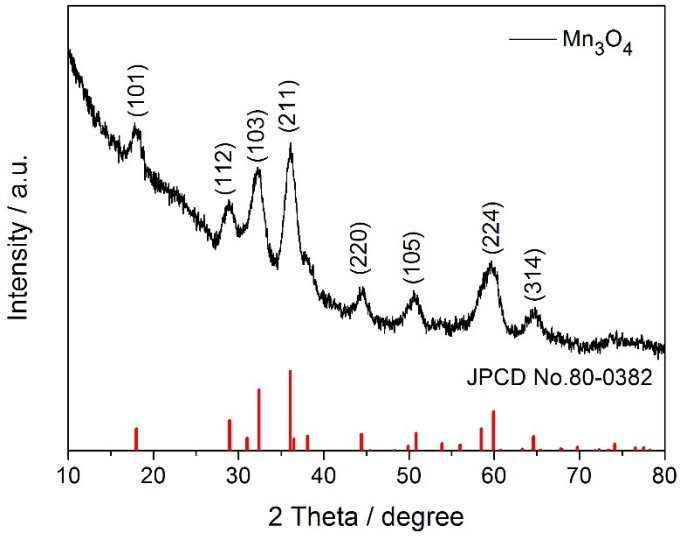

Fig. S3 − XRD pattern of Mn_3O_4 nanoparticles.

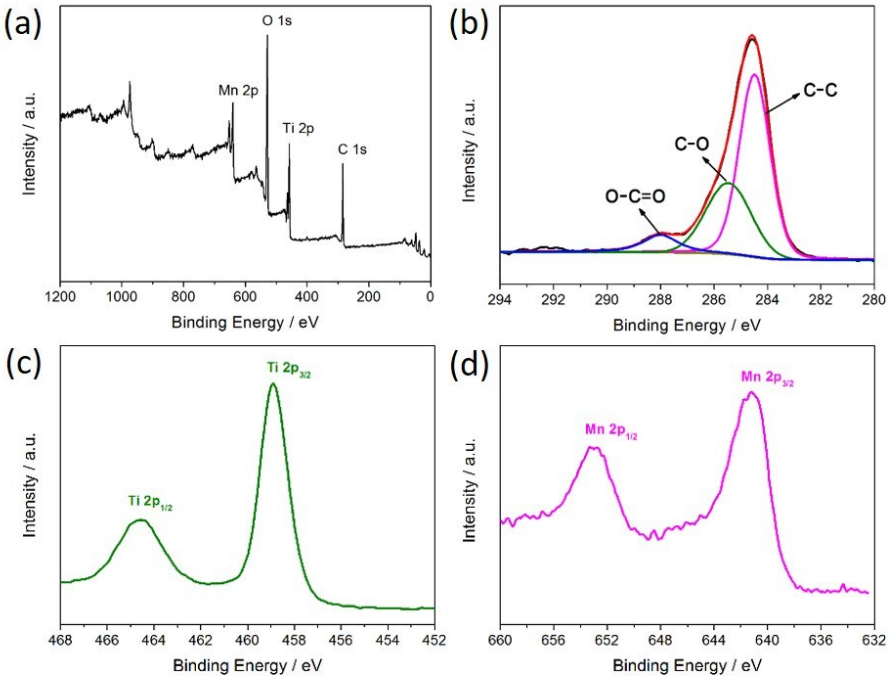

Fig. S4 − (a) Wide-scan survey, (b) C 1s, (c) Ti 2p and (d) Mn 2p XPS spectra of CNT@TiO_2@Mn_3O_4 nanostructures. As to the C1s spectrum, the three peaks located at 284.5, 285.5, and 288.0 eV correspond to the carbon atoms in C-C, C-O, and C=O groups, respectively.[1] In the binding energy of 468-452 eV, the two peaks at 464.6, and 458.9 eV are assigned to Ti $2p_{1/2}$ and $2p_{3/2}$ orbitals.[2] The high-resolution Mn 2p spectrum shows two major peaks residing at 653.0 and 641.2 eV, which are attributed to Mn $2p_{1/2}$ and $2p_{3/2}$ orbitals, indicating that the Mn atoms are in the form of Mn_3O_4. [3]

1 X. Hu, G. Zeng, J. Chen, C. Lu and Z. Wen, *J. Mater. Chem. A*, 2017, **5**, 4535-4542.

2 T. Xia , W. Zhang , J. B. Murowchick , G. Liu , X. Chen , *Adv. Energy Mater*. 2013, **3**, 1516-1523.

3 C. Wang, L. Yin, D. Xiang and Y. Qi, *ACS applied materials & interfaces*, 2012, **4**, 1636-1642.

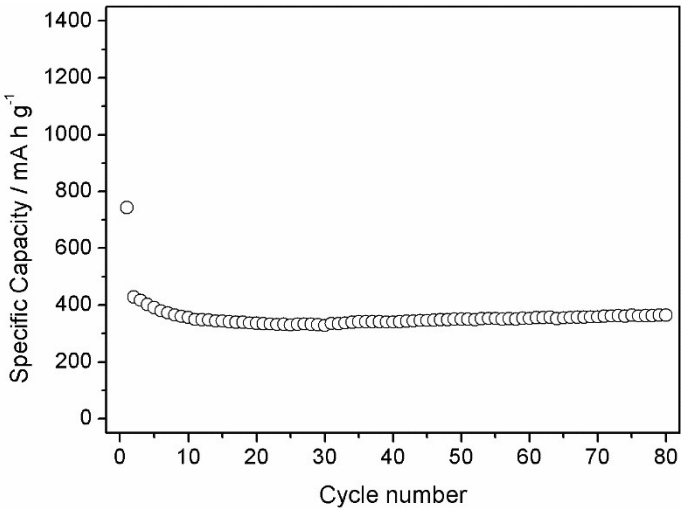

Fig. S5 − Cycle behavior of CNTs at a current density of 500 mA g^{-1}.

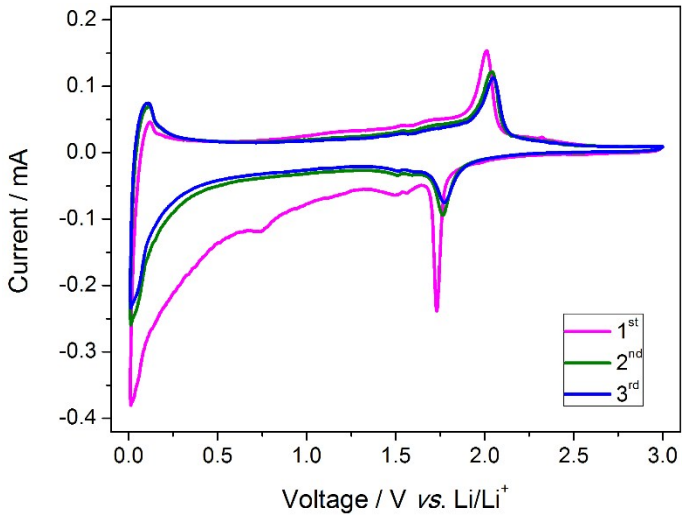

Fig. S6 − Initial three CV curves of CNT@TiO_2 nanostructures.

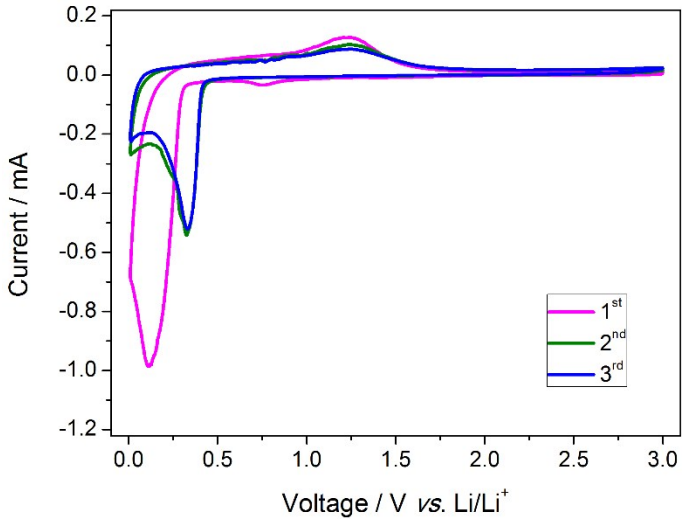

Fig. S7 − Initial three CV curves of Mn_3O_4 nanoparticles.

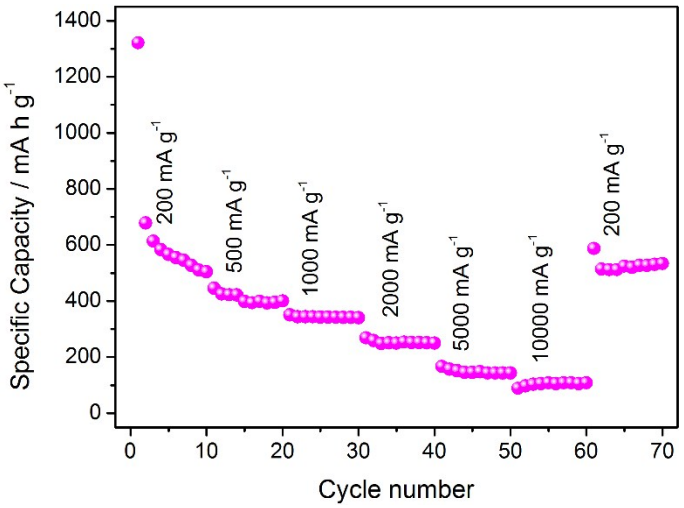

Fig. S8 – Rate capabilities of CNT@TiO_2@Mn_3O_4 nanostructures. A fairly high reversible capacity is witnessed, being 679, 425, 344, 259 or 157 mA h g^{-1} at 200, 500, 1000, 2000 or 5000 mA g^{-1}.When the current density is increased to 10000 mA g^{-1}, the reversible capacity is still as high as 97 mA h g^{-1} . Note that even after deep cycling at 10000 mA g^{-1}, the reversible capacity returns to 514 mA h g^{-1} immediately when the current density is recovered to 200 mA g^{-1}, further confirming good cyclability.

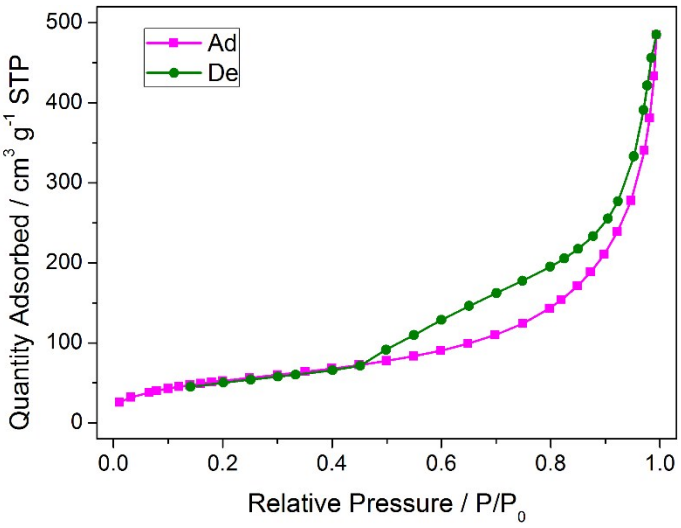

Fig. S9 − Nitrogen adsorption–desorption isotherms of CNT@TiO_2@Mn_3O_4 heteroarchitectures, revealing a large BET surface area of 191.8 m^2 g^{-1} which is favorable for lithium and electrolyte access.

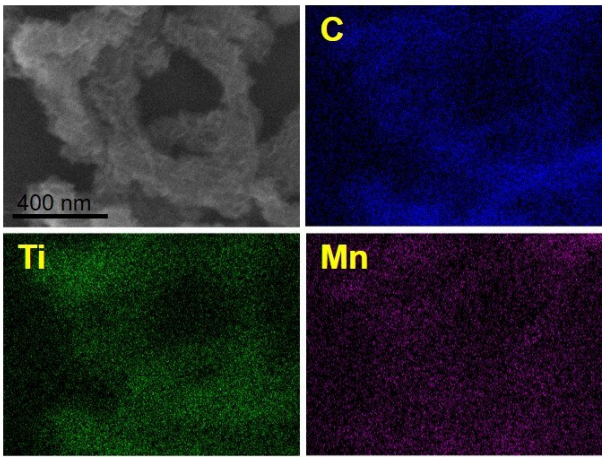

Fig. S10 − SEM image of the CNT@TiO_2@Mn_3O_4 nanostructures after cycling and the corresponding EDS maps of elemental C, Ti and Mn.

Table S1. The content of elemental C in Mn_3O_4, CNT@TiO_2 and CNT@TiO_2@Mn_3O_4 nanostructures

	Mn_3O_4	CNT@TiO_2	CNT@TiO_2@Mn_3O_4
C (wt%)	12.01	27.99	21.64